A SWI/SNF subunit regulates chromosomal dissociation of structural maintenance complex 5 during DNA repair in plant cells

Jieming Jiang[a,1], Ning Mao[a,1], Huan Hu[a], Jiahang Tang[a], Danlu Han[a], Song Liu[a], Qian Wu[a], Yiyang Liu[a], Changlian Peng[a], Jianbin Lai[a,2], and Chengwei Yang[a,2]

[a]Guangdong Provincial Key Laboratory of Biotechnology for Plant Development, School of Life Science, South China Normal University, 510631 Guangzhou, China

Edited by David C. Baulcombe, University of Cambridge, Cambridge, United Kingdom, and approved June 17, 2019 (received for review January 8, 2019)

DNA damage decreases genome stability and alters genetic information in all organisms. Conserved protein complexes have been evolved for DNA repair in eukaryotes, such as the structural maintenance complex 5/6 (SMC5/6), a chromosomal ATPase involved in DNA double-strand break (DSB) repair. Several factors have been identified for recruitment of SMC5/6 to DSBs, but this complex is also associated with chromosomes under normal conditions; how SMC5/6 dissociates from its original location and moves to DSB sites is completely unknown. In this study, we determined that SWI3B, a subunit of the SWI/SNF complex, is an SMC5-interacting protein in *Arabidopsis thialiana*. Knockdown of *SWI3B* or *SMC5* results in increased DNA damage accumulation. During DNA damage, *SWI3B* expression is induced, but the SWI3B protein is not localized at DSBs. Notably, either knockdown or overexpression of *SWI3B* disrupts the DSB recruitment of SMC5 in response to DNA damage. Overexpression of a cotranscriptional activator ADA2b rescues the DSB localization of SMC5 dramatically in the *SWI3B*-overexpressing cells but only weakly in the *SWI3B* knockdown cells. Biochemical data confirmed that ADA2b attenuates the interaction between SWI3B and SMC5 and that SWI3B promotes the dissociation of SMC5 from chromosomes. In addition, overexpression of *SMC5* reduces DNA damage accumulation in the *SWI3B* knockdown plants. Collectively, these results indicate that the presence of an appropriate level of SWI3B enhances dissociation of SMC5 from chromosomes for its further recruitment at DSBs during DNA damage in plant cells.

DNA repair | chromosomal dissociation | plant cells | SMC5/6 | SWI3B

Accurate maintenance of genetic information is essential for the survival of an organism, but DNA damage due to either endogenous processes or exogenous sources reduces genome stability in all cell types (1). Double-strand breaks (DSBs) are a critical form of DNA damage that usually results in defects in replication and transcription (2). Accordingly, several strategies have evolved for response to DSBs, including cell cycle control, apoptosis, and DNA repair (3). Defects of DSB repair disrupt development and underlie many diseases, including cancer (4). Given that the critical components of DSB repair are conserved in eukaryotic cells, studies in model organisms may shed light on the common mechanisms of this process among species.

DSBs are repaired via mechanisms including nonhomologous end joining (NHEJ) and homologous recombination (HR) (5). Unlike NHEJ, which links two ends of broken DNA by direct ligation, HR corrects DSB defects in an error-free manner using the intact homologous region as a template (6). When DNA damage occurs, histone H2AX proteins around the DSB regions are phosphorylated by ATAXIA-TELANGIECTASIA MUTATED (ATM) or ATM/RAD3-RELATED (ATR), and other factors essential in HR repair are also loaded onto DSBs to enable sequential events that include resection, invasion, and resolution (7). During this process, efficient and precise repair relies on the organization and architecture of the chromosomes, with help from the structural maintenance of chromosomes (SMC) proteins (8).

In eukaryotic cells, there are at least six SMC members (SMC1–6) that form three heterodimeric complexes: the cohesin complex (SMC1/3), the condensin complex (SMC2/4), and the SMC5/6 complex (9). All three complexes participate in DNA repair. However, whereas the cohesin and condensin complexes also contribute to the maintenance of chromosome structure in other processes (10), the SMC5/6 complex is required primarily for DNA repair (11). Like the cohesin and condensin complexes, the SMC5/6 complex consists of two SMC members and several non-SMC elements (12). The conserved function of the SMC5/6 complex in HR repair during DNA damage has been observed in different species. For instance, depletion of SMC5/6 components results in sensitivity to ionizing radiation and genotoxic reagents in yeast and animal cells (13, 14). Similarly, in *Arabidopsis*, impaired expression of SMC5/6 complex subunits, including SMC5, SMC6, AtMMS21 (NSE2), NSE1, NSE4, and SNI1, increases the accumulation of DNA damage and has serious effects on development (15–18).

Through yeast two-hybrid screening, we identified SWI3B, a subunit of the SWI/SNF complex involved in chromatin remodeling (19), as an SMC5 interaction partner. The SWI/SNF complex contributes to regulating chromatin accessibility by changing the

Significance

DNA repair is essential for accurate maintenance of genetic information in all types of cells, but what regulatory mechanisms act on the complexes involved in this process has been unclear. The structural maintenance complex 5/6 (SMC5/6) associates with chromosomes under normal conditions and is recruited to DNA double-strand breaks for repair. However, the mechanism by which this conserved complex becomes dissociated from its original chromosomal location during DNA repair is completely unknown. Here, we describe a mechanism in which the chromosomal dissociation of SMC5 in plant cells is mediated via SWI3B, a subunit of the SWI/SNF complex. Given that these proteins are evolutionarily conserved, the current findings may provide hints for the study of DNA repair in other species.

Author contributions: J.J., J.L., and C.Y. designed research; J.J., N.M., H.H., J.T., D.H., S.L., Q.W., and Y.L. performed research; J.J., C.P., J.L., and C.Y. analyzed data; and J.L. and C.Y. wrote the paper.

The authors declare no conflict of interest.

This article is a PNAS Direct Submission.

[1]J.J. and N.M. contributed equally to this work.

[2]To whom correspondence may be addressed. Email: 20141062@m.scnu.edu.cn or yangchw@scnu.edu.cn.

This article contains supporting information online at www.pnas.org/lookup/suppl/doi:10.1073/pnas.1900308116/-/DCSupplemental.

Published online July 8, 2019.

positions of nucleosomes on DNA (20). The conserved core of this complex contains a SWI2/SNF2 ATPase, SWP73, SNF5, and a pair of SWI3 subunits (21). In *Arabidopsis*, there are four SWI3 proteins, which form different dimers and cause functional variation of distinct SWI/SNF complexes (22). However, the functional association of these SWI/SNF subunits with DNA repair has not yet been elucidated in plant cells. SWI3B can form homodimers or heterodimers with other SWI3 proteins (23) and is reported to interact with several proteins involved in different pathways, for instance HAB1 for regulation of ABA signaling and IDN2 for transcriptional silencing (24–26).

The recruitment of the SMC5/6 complex to DSBs is mediated by the BRCT-domain-containing protein RTT107 in yeast cells and by SLF1/2 factors in vertebrate cells (27, 28). We previously found that a conserved transcriptional activator, ADA2b, is essential for recruitment of SMC5 to DSBs in plant cells (29). However, given that the SMC5/6 complex is associated with chromosomes under normal conditions (30), an unanswered question is how this complex moves from regular chromosomal regions to DSBs. In this study, we uncovered a functional association of SWI3B and SMC5, and established a model whereby the movement of SMC5 in response to DNA damage is mediated by SWI3B.

Results

SWI3B Interacts with SMC5 In Vitro and In Vivo. Because the conserved SMC5/6 complex is critical for the maintenance of genome stability in plant cells (15, 16, 31), we performed yeast two-hybrid screening to investigate the interactions between SMC5 and a couple of chromatin-associated components. Our previous study illustrated that ADA2b interacts with SMC5 to recruit the SMC5/6 complex to DSB sites (29). Through a similar assay, we identified SWI3B, a subunit of the SWI/SNF chromatin-remodeling complex, as an SMC5 interaction partner (Fig. 1*A*). We confirmed the physical interaction between SMC5 and SWI3B through an in vitro pull-down assay in which we found that the FLAG-tagged SWI3B protein precipitated with GST-SMC5 but not with a GST-only control (Fig. 1*B*). A further yeast two-hybrid analysis identified the interaction domains, showing that the C-terminal domain of SMC5 specifically interacted with the N-terminal region of SWI3B (Fig. 1 *C* and *D*). When we coexpressed CFP-SWI3B and SMC5-YFP (yellow fluorescent protein) in protoplasts, these two

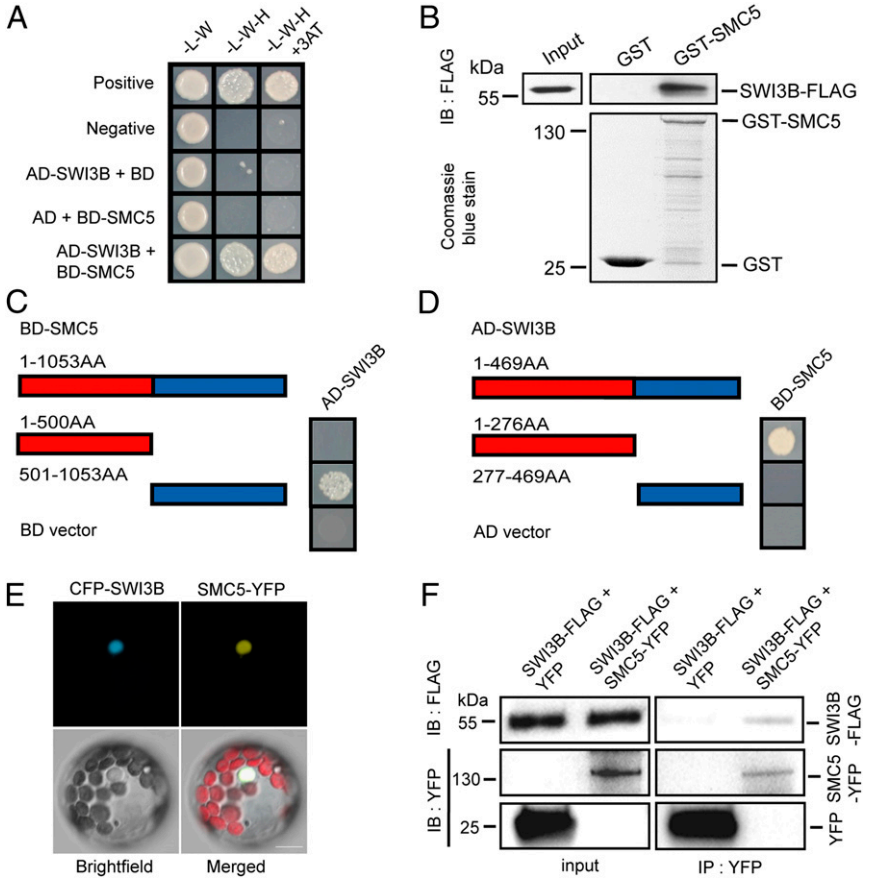

Fig. 1. SWI3B interacts with SMC5 in vitro and in vivo. (*A*) The interaction between SMC5 (fused with the DNA-binding domain, BD) and SWI3B (fused with the activation domain, AD) was detected via yeast two-hybrid assay. (*B*) The interaction between SMC5 and SWI3B was measured in an in vitro pull-down assay. SMC5 was fused with GST and SWI3B was fused with FLAG, and the precipitated SWI3B-FLAG associated with the immobilized GST-SMC5 was detected. The protein levels of GST (control) and GST-SMC5 were visualized via Coomassie blue staining. (*C* and *D*) The domains involved in the SMC5–SWI3B interaction were identified in yeast two-hybrid assays. Detection of the interaction of SWI3B with the N terminus (amino acids 1 to 500) or the C terminus (amino acids 501 to 1053) of SMC5 is shown in (*C*); detection of the interaction of SMC5 with the N terminus (amino acids 1 to 276) or the C terminus (amino acids 277 to 469) of SWI3B is shown in *D*. (*E*) Colocalization of SMC5 and SWI3B in protoplasts. The signals from CFP-SWI3B (in blue), SMC5-YFP (in yellow), bright field (in gray), and merged images are shown. (Scale bar, 10 μm.) (*F*) Detection of in vivo interaction between SMC5 and SWI3B via immunoprecipitation. SWI3B fused with a FLAG tag was coexpressed with SMC5-YFP or YFP (control) in protoplasts. Total protein extracts were immunoprecipitated with immobilized anti-GFP agarose. The precipitated and input signals were detected via immunoblots using a GFP or FLAG antibody. The data in this figure are representative of three independent experiments.

proteins colocalized in the nucleus (Fig. 1*E*), implying a potential for in vivo interaction. We also measured the in vivo association between SWI3B and SMC5 using coimmunoprecipitation by coexpressing SWI3B-FLAG with either free YFP or SMC5-YFP in protoplasts for further analysis. SWI3B-FLAG specifically interacted with SMC5-YFP but not with the YFP control (Fig. 1*F*). Taken together, these results provided evidence of interaction between SMC5 and SWI3B both in vitro and in vivo.

Knockdown of *SWI3B* or *SMC5* Enhances DNA Damage Accumulation. Because our previous study showed that disruption of *SMC5* enhances DNA repair defects in *Arabidopsis* (29), we next investigated whether SWI3B is also involved in DNA damage response. Because knockout of *SMC5* or *SWI3B* results in embryo lethality (15, 22), we used RNA interference (RNAi) to decrease the expression levels of the two genes (26, 29) (*SI Appendix*, Fig. S1). Both the *SWI3B*-RNAi and *SMC5*-RNAi plants displayed similar short-root phenotypes (Fig. 2*A*). Given that impairment of DNA repair could affect root development, we stained the roots of 7-d-old seedlings with propidium iodide (PI) and detected the results via microscopy. Compared with the wild-type plants, plants from the *SWI3B* and *SMC5* knockdown lines had more dead cells in the root meristem regions (Fig. 2*B*), implying that disruption of these genes may result in DNA damage. Furthermore, data from quantitative RT-PCR indicated that the expression levels of genes associated with the DNA damage response, such as *BRCA1*, *PARP2*, and *RAD51*, were increased when either *SWI3B* or *SMC5* was down-regulated (Fig. 2*C*). The results of a comet assay confirmed that DNA damage accumulated significantly in both *SMC5*-RNAi and *SWI3B*-RNAi plants (Fig. 2*D*). Because disruption of DNA repair components may increase sensitivity to DNA damage, we next treated the seedlings with methyl methanesulfonate (MMS), a DNA-damaging reagent. The survival rates confirmed that the *SMC5*-RNAi and *SWI3B*-RNAi plants were more sensitive to MMS than wild-type plants (Fig. 2*E*). These data conclusively supported the possibility that SWI3B and SMC5 are involved in a similar pathway of DNA repair.

SWI3B Is Induced but Not Localized at DSBs During DNA Damage. Upon DNA damage, H2AX is phosphorylated at DSBs for further recruitment of DNA repair components (32). We previously showed that SMC5-YFP colocalizes with phosphorylated H2AX (gamma-H2AX) foci under treatment with MMS (29). Because our results indicated that SWI3B interacts with SMC5, we tested whether SWI3B also localizes at DSBs in response to DNA damage. We first measured the expression of *SWI3B* in response to DNA damage via quantitative RT-PCR. The RNA level of

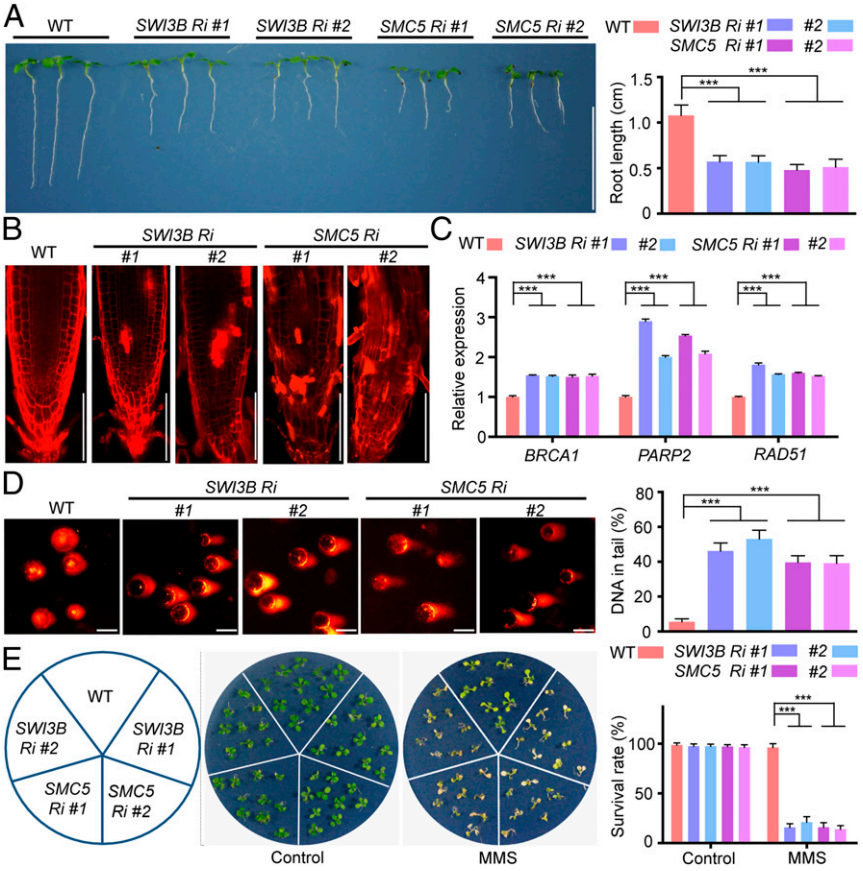

Fig. 2. Knockdown of *SWI3B* or *SMC5* enhances DNA damage accumulation. (*A*) Root development in wild-type (WT), *SWI3B*-RNAi (*SWI3B Ri*), and *SMC5*-RNAi (*SMC5 Ri*) seedlings 7 d after germination. The statistical measurement of root length is shown at *Right*. The data are mean ± SD from at least 30 seedlings in three biological independent experiments. (Scale bar, 1 cm.) (*B*) The meristem regions of 7-d-old roots of the indicated seedlings stained with PI. Dead cells are stained in red. (Scale bars, 100 μm.) (*C*) Expression levels of genes associated with DNA damage, including *BRCA1*, *PAPR2*, and *RAD51*, in 3-wk-old rosette leaves, measured via quantitative RT-PCR. *ACTIN2* was used as an internal control; the expression levels in the wild-type plants were set to 1. The data are mean ± SEM from triplicate experiments. (*D*) DNA damage status monitored in a comet assay. The statistical data for DNA in the comet tail at the right are mean ± SD from three independent biological experiments. (Scale bars, 50 μm.) (*E*) The 5-d-old seedlings were transferred to the medium with or with 100 μg/mL MMS, and photographs were taken 3 d after transfer. The survival rates are mean ± SD from three independent experiments. ***$P < 0.001$, Student's *t* test.

SWI3B was dramatically up-regulated under MMS treatment, and more quickly than that of *ADA2B*, another SMC5-interacting component (Fig. 3*A*). Next, we expressed SWI3B fused with YFP at either its N or C terminus in plant cells. Under normal conditions, both the SWI3B-YFP and YFP-SWI3B proteins were distributed globally in the nucleus. However, different from that of SMC5 (Fig. 3*B*), upon MMS treatment the localization of these SWI3B proteins did not change and no foci were observed in most cells (Fig. 3 *C* and *D*). Even when we increased the concentration of MMS to a high level, the localization pattern of SWI3B was not changed (*SI Appendix*, Fig. S2), suggesting that SWI3B does not localize at DSBs. To assess this conclusion in intact plants, we introduced constructs natively expressing YFP-tagged SMC5 or SWI3B into *smc5* and *swi3b* T-DNA mutants, respectively. The embryo-lethal phenotypes of these mutants were completely rescued, indicating that the YFP-tagged proteins were functional. Both proteins were localized in the nucleus; in addition, when the plants were treated with MMS, SMC5-YFP but not SWI3B-YFP formed foci (*SI Appendix*, Fig. S3), consistent with our conclusion from the protoplast experiments. Our data indicate that SWI3B is not recruited to DSBs during DNA damage.

An Appropriate SWI3B Level Is Important for DSB Localization of SMC5. Given that SWI3B interacts with SMC5 in plant cells, but that the two proteins show different localization in response to MMS treatment, we performed further experiments to uncover the nature of their functional association in response to DNA damage. First, we expressed SMC5-YFP in wild-type and *SWI3B*-RNAi plants. The SMC5-YFP foci appeared in response to MMS in the wild-type cells, consistent with our previous result. However, we did not observe focal localization of SMC5-YFP under MMS treatment in most of the cells generated from the *SWI3B*-RNAi plants (Fig. 3 *E* and *G*), suggesting that SWI3B is important for correct localization of SMC5 at DSBs. The percentage of cells with SMC5-YFP foci was slightly higher in the *SWI3B* knockdown

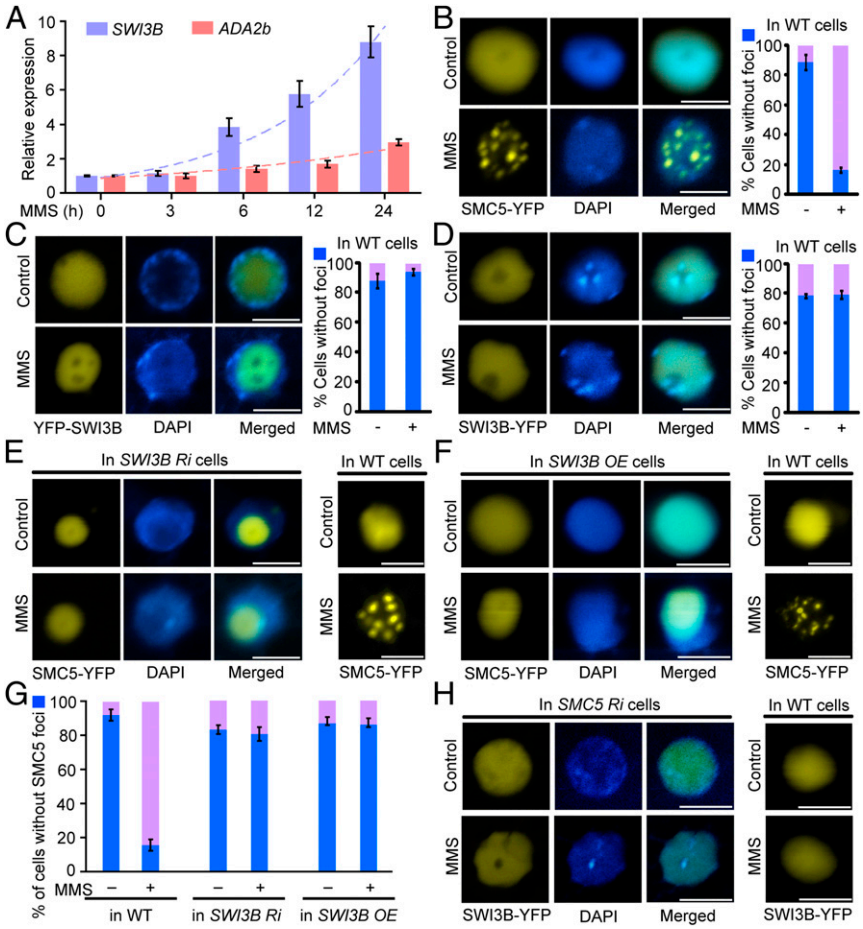

Fig. 3. An appropriate SWI3B level is important for the correct DSB localization of SMC5. (*A*) RNA levels of *SWI3B* and *ADA2b* after MMS treatment detected via quantitative RT-PCR. The 5-d-old seedlings were treated with 100 μg/mL MMS and collected at the indicated time points for RNA extraction. The RNA levels of *SWI3B* and *ADA2b* without MMS treatment were set to 1. The data are mean ± SEM from triplicate experiments. (*B*) Representative localization of SMC5-YFP in protoplasts with or without 100 μg/mL MMS treatment. (*C* and *D*) Representative localization of YFP-SWI3B (*C*) or SWI3B-YFP (*D*) in wild-type protoplasts with or without 100 μg/mL MMS treatment. The quantitative data for the focus formation of SMC5-YFP (*B*), YFP-SWI3B (*C*), and SWI3B-YFP (*D*) are included at the right (*B*–*D*). Percentages of protoplasts with (in purple) or without (in blue) YFP foci are mean ± SD from three independent experiments. (*E* and *F*) Representative localization of SMC-YFP in cells generated from the *SWI3B*-RNAi (*SWI3B Ri*; *E*) or the *SWI3B*-overexpressing (*SWI3B OE*; *F*) plants with or without 100 μg/mL MMS treatment. The localization of SMC5-YFP in wild-type (WT) cells is also shown at the right. (*G*) Histogram data from the wild-type, *SWI3B*-RNAi, and *SWI3B*-overexpressing plants for percentages of protoplasts with (in purple) or without (in blue) SMC5-YFP foci; data are mean ± SD from three independent experiments. (*H*) Representative localization of SWI3B-YFP in cells from the wild-type and *SMC5*-RNAi plants with or without 100 μg/mL MMS treatment. In all of the microscopy images in this figure, the signals from YFP (in yellow), DAPI (in blue, for nucleus staining), and the merged images are shown. The quantitative data in this figure for the percentages of cells with or without foci are mean ± SD from three independent experiments (at least 100 cells were detected in each sample). (Scale bars, 5 μm.)

cells than in wild-type cells, even under normal conditions (Fig. 3*G*), possibly as a result of a higher level of DNA damage response. In addition, because SMC5 and SWI3B displayed different localization under MMS treatment, we explored what happened when both were overexpressed. Surprisingly, when SMC5-YFP was coexpressed with CFP-SWI3B, no focus formation was detected for either protein in most of cells (*SI Appendix*, Fig. S4), implying that overexpression of SWI3B interferes with the DSB localization of SMC5. We confirmed this conclusion in another experiment by measuring the localization of SMC5-YFP in the transgenic *SWI3B*-overexpressing plants (Fig. 3 *F* and *G*). Conversely, when we expressed YFP-SWI3B in protoplasts generated from the wild-type or *SMC5*-RNAi plants with or without MMS, we found that the nucleus localization of SWI3B was not affected by disruption of *SMC5* expression (Fig. 3*H*). Given that the focal localization of SMC5 was disturbed when *SWI3B* was either knocked down or overexpressed, and that both knockdown and overexpression of *SWI3B* resulted in increased sensitivity to MMS (Fig. 2*E* and *SI Appendix*, Fig. S5), it seems possible that an appropriate level of SWI3B (neither too high nor too low) is critical for the localization of SMC5 during DNA damage.

ADA2b Rescues DSB Localization of SMC5 in *SWI3B*-Misexpressing Cells. Our previous study showed that ADA2b is essential for recruitment of SMC5 at DSBs (29); therefore, we analyzed the effect of ADA2b on the functional association between SWI3B and SMC5. When we expressed YFP-ADA2b in protoplasts generated from the *SWI3B*-RNAi (Fig. 4*A*) or *SWI3B*-overexpressing (Fig. 4*B*) transgenic plants, YFP-ADA2b was distributed globally in the nucleus under the control condition and was predominantly recruited to DSBs in response to MMS, similar to its localization pattern in wild-type cells (*SI Appendix*, Fig. S6). We also verified the DSB localization of ADA2b in these cells by immunohistochemistry using the antibody against gamma-H2AX, a marker for DSBs (*SI Appendix*, Fig. S7). The results confirmed that neither overexpression nor knockdown of *SWI3B* has any effect on the DSB recruitment of ADA2b.

To elucidate the effect of ADA2b on SMC5 recruitment in the *SWI3B*-misexpressing cells, we cotransformed the *SMC5-YFP* plasmid with increasing amounts of *mCherry-ADA2b* (the ratio of plasmid concentration between *mCherry-ADA2b* and *SMC5-YFP* was 0, 1, 2, 4, or 8) in the *SWI3B*-overexpressing or knockdown cells. In the *SWI3B*-overexpressing protoplasts, when SMC5-YFP was expressed alone MMS did not change the localization pattern of SMC5-YFP, and when ADA2b was coexpressed the percentages of cells with SMC5-YFP foci in response to MMS were dramatically increased (2×ADA2b was enough to rescue the foci formation of SMC5-YFP in the majority of cells) (Fig. 4 *C* and *D*). In the *SWI3B*-RNAi cells, when SMC5-YFP was coexpressed with mCherry-ADA2b the percentages of cells with SMC5-YFP foci increased much more weakly as the ADA2b level increased (2×ADA2b had no significant effect on the localization pattern of SMC5-YFP; even 8×ADA2b was not enough to completely restore the DSB localization of SMC5-YFP) (Fig. 4 *E* and *F*), compared with those in the *SWI3B*-overexpressing cells. In the *SWI3B*-RNAi cells, SMC5 may be maintained on chromosomes without the assistance of SWI3B; therefore, an excess of ADA2b is not enough to enhance the complete dissociation of SMC5 from chromosomes for further DSB recruitment.

SWI3B Promotes Dissociation between SMC5 and Chromosomes. Because SWI3B does not localize to DSBs, its interaction with SMC5 may block the correct recruitment of SMC5. This possibility is consistent with our data indicating that ADA2b overexpression dramatically enhances the formation of SMC5-YFP foci in *SWI3B*-overexpressing cells (Fig. 4 *C* and *D*). Furthermore, when we used a competition assay to measure the effect of ADA2b on the SMC5-SWI3B interaction, we found that increasing amounts of ADA2b-FLAG attenuated the affinity between GST-SWI3B and SMC5-YFP (Fig. 4*G*), providing evidence of direct competition between ADA2b and SWI3B for interaction with SMC5.

However, it is more difficult to understand why knockdown of *SWI3B* also disrupts the localization of SMC5 under MMS treatment. Given that SMC5 may be globally associated with chromosomes under normal conditions (33), if SWI3B is important for its dissociation from chromosomes for further DSB recruitment, knockdown of *SWI3B* might result in maintenance of SMC5 in its original chromosomal locations. This may also be why overexpression of *ADA2b* only weakly rescues the DSB localization of SMC5-YFP in the *SWI3B*-RNAi cells (Fig. 4 *E* and *F*). Therefore, we assessed the association of SMC5 with chromosomes via a coimmunoprecipitation assay between SMC5 and the DNA-bound H3, a regular histone subunit generally distributed on chromosomes. SMC5 was associated with H3 with DNA fragments, but this association was reduced in the presence of abundant SWI3B (Fig. 4*H*), supporting the idea that SWI3B interferes with the interaction between SMC5 and chromosomes. The increased level of SWI3B may enhance the dissociation of SMC5 from its original chromosomal location, making it available for further ADA2b-mediated recruitment at DSBs.

Excess SMC5 Reduces DNA Damage Accumulation in the *SWI3B*-RNAi Plants. Our data indicated that SMC5 was mislocalized in the *SWI3B*-RNAi plants, possibly as a result of their defect in the dissociation of SMC5 from chromosomes. Therefore, we overexpressed *SMC5* in the *SWI3B*-RNAi plants to detect the effect of excess SMC5 in these plants and found that the root developmental defect of the *SWI3B*-RNAi plants was rescued by *SMC5* overexpression (Fig. 5 *A* and *C*). The results from a comet assay also indicated that overexpression of *SMC5* in the *SWI3B*-RNAi plants reduced DNA damage accumulation (Fig. 5 *B* and *C*). Moreover, in the early stage of root development, overexpression of *SMC5* suppressed cell death and attenuated MMS sensitivity in the root meristems of *SWI3B*-RNAi plants (Fig. 5*D*). The survival rate of the *SWI3B*-RNAi seedlings under MMS treatment was also partially rescued by overexpression of *SMC5* (*SI Appendix*, Fig. S8). We also measured the DSB recruitment of transiently expressed SMC5-YFP in cells generated from these transgenic plants. Compared with the results from the *SWI3B*-RNAi cells, formation of the SMC5-YFP foci was significantly enhanced in response to MMS in the cells generated from the *SWI3B*-RNAi/*SMC5*-overexpressing transgenic plants (Fig. 5*E*). Therefore, when *SMC5* is overexpressed, the excess SMC5 may be free to move without chromosomal association under normal conditions; when DNA damage occurs, the free SMC5 proteins can then be recruited at DSBs in a proportion of cells to act in DNA repair, without chromosomal dissociation mediated by SWI3B.

Discussion

Upon DNA damage, several protein factors, such as RTT107, SLF1/2, and ADA2b, work as mediators for the SMC5/6 recruitment at DSBs in different species (27–29). In addition, the subunits of this complex, such as NSE1 and NSE3, also contribute to its chromosomal association (34, 35). Studies of the regulatory mechanisms of SMC5/6 recruitment have generally focused on the function of adaptors at DSBs (36). Because this complex is also globally associated with chromosomes under normal conditions (37), however, the first step in its relocalization is likely the dissociation from its original chromosomal location, but to date no factors had been characterized as being involved in this process. Here, we identified an SMC5-interacting protein, SWI3B, in plant cells and demonstrated that this component enhances the dissociation of SMC5 from chromosomes, making them available for further DSB recruitment in response to DNA damage.

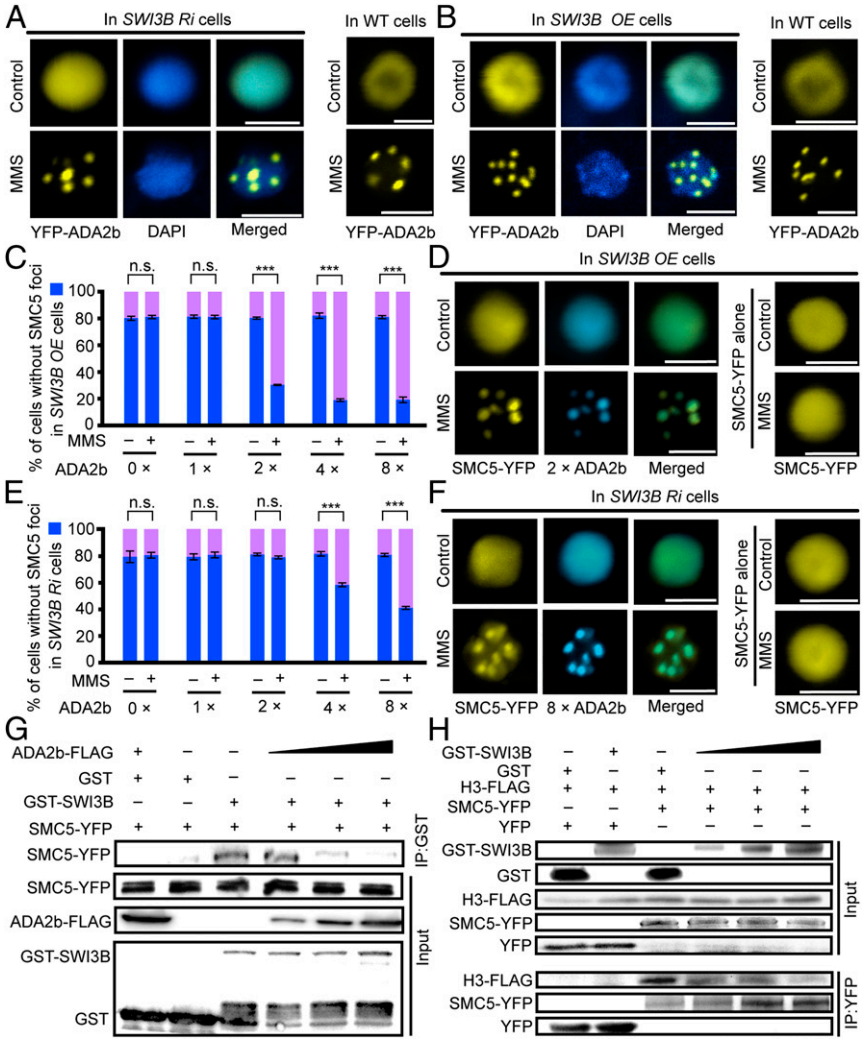

Fig. 4. ADA2b rescues the DSB localization of SMC5 in the *SWI3B*-misexpressing cells. (*A* and *B*) Representative localization of YFP-ADA2b in cells generated from *SWI3B*-RNAi (*SWI3B Ri*; *A*) and *SWI3B*-overexpressing (*SWI3B OE*; *B*) plants with or without 100 μg/mL MMS treatment. The localization of YFP-ADA2b in the wild-type (WT) cells is also shown at the right. The quantitative data are provided in *SI Appendix*, Fig. S6. (*C*–*F*) SMC5-YFP was coexpressed with increasing levels of mCherry-ADA2b in *SWI3B*-overexpressing or *SWI3B*-RNAi cells with or without 100 μg/mL MMS treatment (with ratios of plasmid concentrations between *mCherry-ADA2b* and *SMC5-YFP* of 0, 1, 2, 4, or 8). The histogram data for the effect of *mCherry-ADA2b* (0×, 1×, 2×, 4×, and 8×) on the percentages of cotransfected cells with (in purple) or without (in blue) SMC5-YFP foci are mean ± SD from three independent experiments (at least 100 cells were detected in each sample). The quantitative data from the *SWI3B*-overexpressing samples are shown in *C*; the quantitative data from the *SWI3B*-RNAi samples are shown in *E*. ***$P < 0.001$; n.s., no significance; Student's *t* test. Representative localization of SMC5-YFP and mCherry-ADA2b (2×) in the *SWI3B*-overexpressing cells is shown in *D*; the representative localization of SMC5-YFP and mCherry-ADA2b (8×) in the *SWI3B*-RNAi cells is shown in *F*. (Scale bars, 5 μm.) (*G*) ADA2b competes with SWI3B for SMC5 binding. GST-SWI3B, GST (control), SMC-YFP, or ADA2b-FLAG was expressed in *E. coli* for further protein extraction. The precipitated SMC5-YFP associated with the immobilized GST-SWI3B was measured in an in vitro pull-down assay. Increasing amounts of ADA2b-FLAG were added to the system to detect the effect of ADA2b on the interaction between SMC5 and SWI3B. (*H*) SWI3B enhances the dissociation of SMC5 from chromosomes. H3-FLAG was expressed in protoplasts, and DNA was fragmented using micrococcal nuclease. The total lysate with SMC5-YFP or YFP was precipitated with immobilized anti-GFP agarose. Purified GST or GST-SWI3B from *E. coli* was added to the system, and the effect of the increased level of GST-SWI3B on the association between SMC5-YFP and histone H3 was detected. The images are representative of three independent experiments.

SWI3B is a subunit of the SWI/SNF chromatin remodeling complex (22), which is involved in the regulation of various biological processes in plant cells (38), but its function in DNA repair was unknown. Our data show that DNA damage accumulation is significantly increased when *SWI3B* is knocked down (Fig. 2), suggesting that this component might play a role in the DNA damage response pathway. Our previous screening showed that SMC5 does not interact with SWI3C (29), another subunit in the SWI/SNF complex, implying that not all SWI3 subunits are involved in this process. In addition, SWI3B alone interferes with the interaction between SMC5 and chromosomes, suggesting that this process may not be mediated by chromatin remodeling. Previous studies had shown that the SWI/SNF complex is involved in DNA repair in mammalian cells (39). For instance, the ATP-dependent remodeler BRG1 regulates the chromosome structure near DSBs to allow further access of the DNA repair machinery in human cells (40), suggesting that the SWI/SNF complex may have a direct function in this process (41), but whether the complex also directly participates in DNA repair in plant cells needs further investigation.

Unlike ADA2b, which is essential for correct recruitment of SMC5 at DSBs during DNA damage (29), SWI3B does not localize at DSBs upon treatment with DNA-damaging agents, but it is important for the localization of SMC5. Our results also

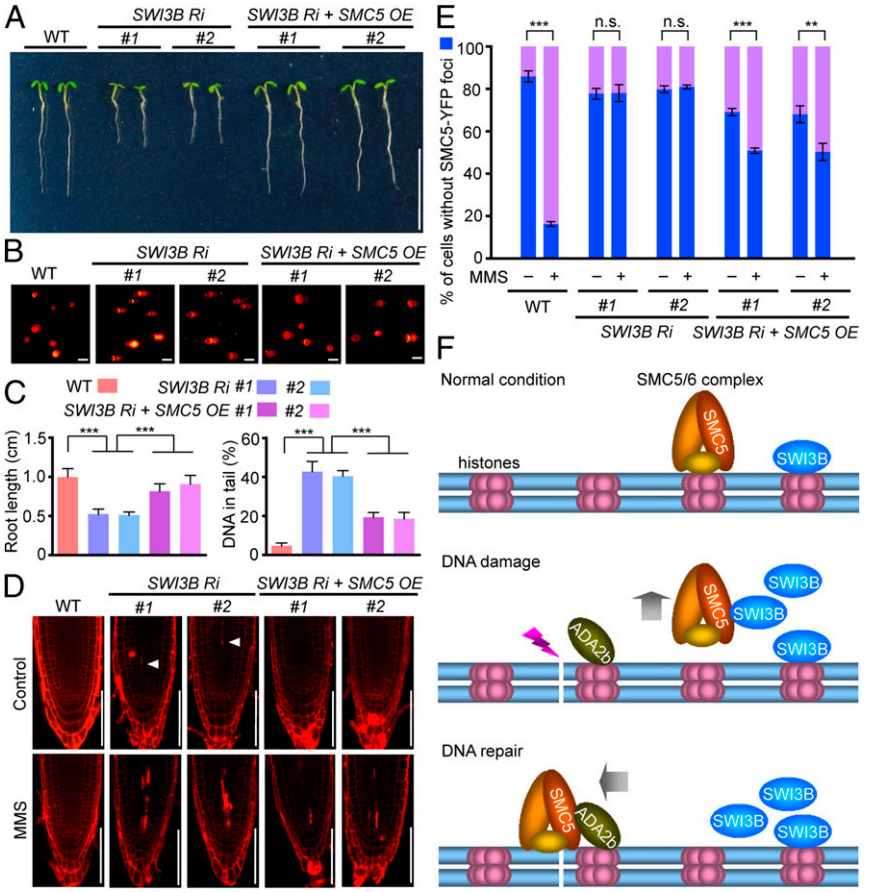

Fig. 5. Excess SMC5 reduces DNA damage accumulation in the *SWI3B*-RNAi plants. (*A*) Effect of *SMC5* overexpression on the root development of *SWI3B*-RNAi (*SWI3B Ri*) seedlings of different genotypes. The photograph was taken 6 d after germination. (Scale bar, 1 cm.) (*B*) DNA damage status of indicated 3-wk-old plants monitored in a comet assay. (Scale bars, 10 μm.) (*C*) Statistical analysis of root length and DNA in tail in the comet assay. The root length data are mean ± SD from at least 30 seedlings. The data from the comet assay are from three independent experiments. ***$P < 0.001$, Student's *t* test. (*D*) The roots of 4-d-old plants were treated with or without 75 μg/mL MMS for 1 d and then the root meristem regions of the indicated seedlings were stained with PI. The initiation of cell death in the control condition is indicated by arrowheads. (Scale bars, 100 μm.) (*E*) SMC5-YFP was expressed in protoplasts generated from wild-type (WT), *SWI3B*-RNAi (*SWI3B Ri*), and *SWI3B*-RNAi/*SMC5*-overexpressing (*SWI3B Ri* + *SMC5 OE*) plants with or without 100 μg/mL MMS treatment. The histogram data from the indicated plants for the percentages of protoplasts with (in purple) or without (in blue) SMC5-YFP foci are mean ± SD from three independent experiments. ***$P < 0.001$; **$P < 0.01$; n.s., no significance; Student's *t* test. (*F*) A model for chromosomal dissociation and DSB recruitment of SMC5 mediated via SWI3B and ADA2b in plant cells.

showed that the DSB localization of ADA2b is independent of SWI3B, suggesting that SMC5 recruitment may be directly mediated by SWI3B (Fig. 4 *A* and *B*). The dynamic localization of chromatin-associated proteins, such as histones, requires other exchange factors for their dissociation with chromosomes (42). In yeast and mammalian cells, the SMC5/6 complex is associated with chromosomes under normal conditions (33). Therefore, SWI3B may play a role in the chromosomal dissociation of SMC5 before it localizes to DSBs, and this possibility is supported by our result that SWI3B interferes with the association between SMC5 and DNA-bound histone H3 (Fig. 4*H*). When *SWI3B* is down-regulated, SMC5 may remain in its original association with a chromosomal region and be unable to move to DSBs when DNA damage occurs, resulting in increased damage accumulation. This conclusion is also supported by the fact that overexpression of ADA2b only weakly restores the DSB localization of SMC5 in *SWI3B*-RNAi cells (Fig. 4 *E* and *F*). Without SWI3B, ADA2b alone is insufficient to dissociate SMC5 from chromosomes for further recruitment to DSBs. The mild effect of a high level of ADA2b on SMC5-YFP recruitment in *SWI3B*-RNAi cells may be a result of a small proportion of free SMC5 being directed to DSBs, due to the effect of excess ADA2b on equilibrium of the free and chromosomal-associated SMC5. In addition, compared with that in the *SWI3B*-RNAi cells, the DSB localization of SMC5-YFP in response to MMS is enhanced in protoplasts generated from the *SWI3B*-RNAi/*SMC5*-overexpressing transgenic plants (Fig. 5*E*). Therefore, in the *SWI3B* knockdown plants, a small amount of free SMC5 molecules resulted from overexpression, without the assistance of SWI3B for chromosomal dissociation, may be enough to participate further DNA repair in a proportion of cells.

When DNA damage occurs, the expression of *SWI3B* is quickly increased, and this enhances the dissociation between SMC5 and chromosomes, releasing free SMC5 in the nucleus. ADA2b, another SMC5-interacting protein, is then sequentially induced (Fig. 3*A*). Given that both SWI3B and ADA2b bind to the C-terminal domain of SMC5, the increased ADA2b may compete with SWI3B for SMC5 binding, a possibility that is supported by the results of our protein competition assay (Fig. 4*G*). Furthermore, overexpression of *ADA2b* dramatically increases DSB localization of SMC5 in the *SWI3B*-overexpressing cells (Fig. 4 *C* and *D*). Therefore, after its SWI3B-mediated dissociation from chromosomes, SMC5 is wrested by ADA2b for further recruitment to DSBs (Fig. 5*F*), consistent with the previous

conclusion that both ADA2b and SMC5 localize at DSBs and that the DSB localization of SMC5 is dependent on ADA2b (29). When SWI3B is overexpressed, there are not enough ADA2b molecules to compete with SWI3B for SMC5 binding, resulting in mislocalization of SMC5 during DNA damage.

Collectively, the results from this study illustrate a mechanism regulating the movement of the SMC5/6 complex during DNA repair in plant cells. SMC5/6 is reported to be associated with the E2F/DP complex, thereby connecting cell cycle regulation and DNA repair (43–45). Given that SWI3B is a subunit of the SWI/SNF complex, it will be of interest to investigate whether SWI3B also connects two critical complexes, SWI/SNF and SMC5/6, for regulation of gene transcription and DNA repair. Given that SWI3B, ADA2b, and SMC5 are highly conserved proteins, from yeast to human and plant cells, and their association was not previously known, it will be valuable to investigate whether these functional connections exist in other species, as answers to this question may improve understanding of the general mechanisms of DNA repair.

Materials and Methods

Plant Materials and Growth Condition. Seeds were surface-sterilized for 2 min in 75% ethanol and 6 min in 2.5% NaClO solution, rinsed six times with sterile water, and plated on Murashige and Skoog (MS) medium with 1.5% sucrose and 1% agar and stratified at 4 °C in the dark for 2 d, then transferred into a greenhouse at 21 °C in a light/dark cycle of 16 h/8 h. For MMS treatment assay, 5-d-old seedlings were transferred to MS medium with or without 100 μg/mL MMS (129925; Sigma) for 3 d before being scored and photographed.

Yeast Two-Hybrid Assay. For the yeast two-hybrid assay, the coding sequence (CDS) regions of *SMC5* and *SWI3B* were cloned into the *pGBKT7* vector and *pGADT7* vector, respectively. For characterizing the interaction domains, the truncated sequences were generated as described in the figure legends. The experiments were conducted by the manufacturer's instructions for the Matchmaker GAL4-based Two-hybrid System 3 (Clontech). The interactions were selected stringently with SD/–Leu/–Trp/–His minimal medium supplied with 3-amino-1,2,4-triazole.

In Vitro Pull-Down Assay. To detect the interaction between SMC5 and SWI3B, the CDS of *SMC5* was fused into vector *pGEX4T-1*, and the *SWI3B* was cloned into vector *pET28a* with a FLAG tag. The recombinant vectors were transferred into the *BL21* strain, respectively. The extracts from bacteria expressing GST or GST-SMC5 were incubated with glutathione Sepharose (GE Healthcare) for 30 min at room temperature in a binding buffer (50 mM Tris, pH 7.4, 120 mM NaCl, 5% glycerol, 0.5% Nonidet P-40, 1 mM PMSF, and 1 mM β-mercaptoethanol). The resins then was collected for further incubation with extraction from bacterial expressing SWI3B-FLAG at room temperature for 60 min. After rinsing using washing buffer (50 mM Tris, pH 7.4, 120 mM NaCl, 5% glycerol, and 0.5% Nonidet P-40) five times, the Sepharose was mixed with SDS sample buffer and boiled for SDS/PAGE and immunoblots. To determine the effect of ADA2b on the interaction between SMC5 and SWI3B, the SMC-YFP protein was extracted and incubated with GST, GST-SWI3B on glutathione Sepharose. ADA2b-FLAG expressed from bacteria was added in the system. Other procedures were similar to those given in the description above.

Coimmunoprecipitation. For coimmunoprecipitation between SMC5 and SWI3B, the CDS of *SMC5* was cloned into the vector *pSAT6-EYFP-N1* to generate a *35S:SMC5-YFP* plasmid. The CDS of *SWI3B* was fused with a FLAG tag and cloned into a *pBluescript*-based vector (44) to generate *35S:SWI3B-FLAG* plasmid. The *35S:SWI3B-FLAG* was cotransformed with *35S:SMC5-YFP* or *35S:YFP* (control) into protoplasts (46). Protoplasts were harvested after 48 h and resuspended in the extraction buffer (10 mM Tris·HCl, pH 7.4, 100 mM NaCl, 10% glycerol, and 0.5% Nonidet P-40) containing protease inhibitor mixture (Roche). After it was spun down, the supernatant was incubated with the GFP-Trap resin for 3 h at 4 °C. Then the resin was collected and washed 3 times with the washing buffer (10 mM Tris·HCl, pH 7.4, 100 mM NaCl, and 10% glycerol). The proteins were eluted with the SDS sample buffer and subjected for immunoblot using anti-GFP (Abcam) or anti-FLAG (Sigma) antibodies.

For detection of association between SMC5 and DNA-bound histone H3, the H3-FLAG protein was expressed in protoplasts, the extract in lysis buffer (10 mM Tris·HCl, pH 7.4, 100 mM NaCl, 10% glycerol, and 0.5% Nonidet P-40) with protease inhibitor mixture for 1 h at 4 °C, and DNA was fragmented via treatment with Micrococcal Nuclease (M0247S, 5 μL for 4×10^7 cells; NEB) for 4 min at 37 °C and EGTA was added to stop reaction. The DNA fragmentation was confirmed by electrophoresis. The DNA-bound H3 samples with YFP or SMC5-YFP was then subjected for incubation with GFP-Trap resin at 4 °C for 30 min. The GST or GST-SWI3B expressed from *Escherichia coli* was then added to the system and incubated at room temperature for 1 h to detect the effect of SWI3B on the interaction between SMC5 and H3.

Generation of Transgenic Plants. The generation of transgenic lines of *SMC5*-RNAi, *35S:SMC5*, and *SWI3B*-RNAi has been described previously (26, 29). To obtain the *SMC5* and *SWI3B* complementation plants, the genomic region of *SMC5* or *SWI3B* with a native promoter was fused with YFP and cloned into *pCambia1300-221*. The constructs were transformed into Agrobacterium *EHA105* and were used for complementation of the heterozygous T-DNA lines of *smc5-2* (*SALK_092081*) and *swi3b* (*CS370196*) by the floral-dip method (47).

Comet Assay. The rosette leaves from 3-wk-old plants were used for comet assays. Comet assays were performed using the Comet Assay Kit from Trevigen (4250-050-K). SYBR Gold from Life Technologies was used for staining. Photographs were captured by the Zeiss LSM 800 confocal microscope with excitation/emission wavelengths of 488 nm/505 to 530 nm and analyzed by Comet Assay Software Project.

Fluorescence Microscopy. For measurement of the localization of SWI3B and SMC5, the CDS of SWI3B was cloned into the *35S:CFP/YFP* vector based on *pBluescript*, and the CDS of SMC5 was cloned into the *pSAT6-EYFP-N1* vector. Generation of the plasmid for expression of YFP-ADA2b was described previously (29). The *mCherry-ADA2b* plasmid was constructed by cloning the genomic region of *ADA2b* into the *pBI221-mCherry* vector. The plasmids were transformed into protoplasts (46) and the fluorescence was detected after 24 h using confocal microscopy. For MMS treatment, protoplasts were incubated in W5 medium with MMS (129925; Sigma). DAPI (D9542; Sigma) was used for nucleus labeling. For confocal laser imaging of roots, roots were counterstained with 10 μg/mL PI (Sigma) for 1 min and mounted in water for observation. Photographs were captured using the Zeiss LSM 800 confocal microscope. Immunofluorescence staining in *SI Appendix*, Fig. S7 was performed following the protocol described previously (29). A primary antibody against gamma-H2AX (48) and an Alexa Fluor 555-coupled goat anti-rabbit antibody (Bioss) were used.

RNA Extraction and Gene Expression Analysis. Total RNA of different genotype plants was extracted from the rosette leaves of 3-wk-old seedlings by using the Plant RNAprep Pure Kit with DNaseI treatment following the manufacturer's instructions and subjected to reverse transcribed using a PrimeScript RT Reagent Kit (Takara). RT-qPCR was then carried out using SYBR Premix Ex Taq (Takara) in a Bio-Rad CFX 96 system (C1000 Thermal Cycler) and detected by Bio-Rad CFX Manager software (Bio-Rad).

Accession Numbers. Sequence data from this article can be found in the *Arabidopsis* Genome Initiative (https://www.arabidopsis.org/) (49) or GenBank/EMBL databases (https://www.ncbi.nlm.nih.gov/; https://www.embl.org/) (50, 51) under the following accession numbers: *SMC5* (*AT5G15920*), *SWI3B* (*AT2G33610*), *ADA2b* (*AT4G16420*), *PARP2* (*AT4G02390*), *BRCA1* (*AT4G21070*), *RAD51* (*AT5G20850*), and *ACTIN2* (*AT3G18780*).

ACKNOWLEDGMENTS. We thank Arabidopsis Biological Resource Center for the mutant seeds used in this study and Professor Frederic Berger (Gregor Mendel Institute) for the gamma-H2AX antibody. This work was supported by grants from the National Natural Science Foundation of China (31871222, 31670286, 31771504, and 31400314); the Natural Science Foundation of Guangdong (2018B030308002); the Guangdong YangFan Innovative and Entrepreneurial Research Team Project (2015YT02H032); and the Guangzhou Scientific and Technological Program (201607010377); and the award from the Program for Changjiang Scholars.

1. O. D. Schärer, Chemistry and biology of DNA repair. *Angew. Chem. Int. Ed. Engl.* **42**, 2946–2974 (2003).
2. R. Ceccaldi, B. Rondinelli, A. D. D'Andrea, Repair pathway choices and consequences at the double-strand break. *Trends Cell Biol.* **26**, 52–64 (2016).
3. S. P. Jackson, J. Bartek, The DNA-damage response in human biology and disease. *Nature* **461**, 1071–1078 (2009).
4. T. Aparicio, R. Baer, J. Gautier, DNA double-strand break repair pathway choice and cancer. *DNA Repair (Amst.)* **19**, 169–175 (2014).

5. J. R. Chapman, M. R. Taylor, S. J. Boulton, Playing the end game: DNA double-strand break repair pathway choice. *Mol. Cell* **47**, 497–510 (2012).
6. M. Jasin, R. Rothstein, Repair of strand breaks by homologous recombination. *Cold Spring Harb. Perspect. Biol.* **5**, a012740 (2013).
7. C. P. Spampinato, Protecting DNA from errors and damage: An overview of DNA repair mechanisms in plants compared to mammals. *Cell. Mol. Life Sci.* **74**, 1693–1709 (2017).
8. A. Seeber, S. M. Gasser, Chromatin organization and dynamics in double-strand break repair. *Curr. Opin. Genet. Dev.* **43**, 9–16 (2017).
9. F. Uhlmann, SMC complexes: From DNA to chromosomes. *Nat. Rev. Mol. Cell Biol.* **17**, 399–412 (2016).
10. A. J. Wood, A. F. Severson, B. J. Meyer, Condensin and cohesin complexity: The expanding repertoire of functions. *Nat. Rev. Genet.* **11**, 391–404 (2010).
11. M. Diaz, A. Pecinka, Scaffolding for repair: Understanding molecular functions of the SMC5/6 complex. *Genes (Basel)* **9**, E36 (2018).
12. N. Wu, H. Yu, The Smc complexes in DNA damage response. *Cell Biosci.* **2**, 5 (2012).
13. H. M. Verkade, S. J. Bugg, H. D. Lindsay, A. M. Carr, M. J. O'Connell, Rad18 is required for DNA repair and checkpoint responses in fission yeast. *Mol. Biol. Cell* **10**, 2905–2918 (1999).
14. P. R. Potts, M. H. Porteus, H. Yu, Human SMC5/6 complex promotes sister chromatid homologous recombination by recruiting the SMC1/3 cohesin complex to double-strand breaks. *EMBO J.* **25**, 3377–3388 (2006).
15. K. Watanabe *et al*., The STRUCTURAL MAINTENANCE OF CHROMOSOMES 5/6 complex promotes sister chromatid alignment and homologous recombination after DNA damage in Arabidopsis thaliana. *Plant Cell* **21**, 2688–2699 (2009).
16. P. Xu *et al*., AtMMS21, an SMC5/6 complex subunit, is involved in stem cell niche maintenance and DNA damage responses in Arabidopsis roots. *Plant Physiol.* **161**, 1755–1768 (2013).
17. G. Li *et al*., Non-SMC elements 1 and 3 are required for early embryo and seedling development in Arabidopsis. *J. Exp. Bot.* **68**, 1039–1054 (2017).
18. S. Yan *et al*., Salicylic acid activates DNA damage responses to potentiate plant immunity. *Mol. Cell* **52**, 602–610 (2013).
19. S. K. Han, M. F. Wu, S. Cui, D. Wagner, Roles and activities of chromatin remodeling ATPases in plants. *Plant J* **83**, 62–77 (2015).
20. C. Y. Zhou, S. L. Johnson, N. I. Gamarra, G. J. Narlikar, Mechanisms of ATP-dependent chromatin remodeling motors. *Annu. Rev. Biophys.* **45**, 153–181 (2016).
21. A. Jerzmanowski, SWI/SNF chromatin remodeling and linker histones in plants. *Biochim. Biophys. Acta* **1769**, 330–345 (2007).
22. T. J. Sarnowski *et al*., SWI3 subunits of putative SWI/SNF chromatin-remodeling complexes play distinct roles during Arabidopsis development. *Plant Cell* **17**, 2454–2472 (2005).
23. T. J. Sarnowski, S. Swiezewski, K. Pawlikowska, S. Kaczanowski, A. Jerzmanowski, AtSWI3B, an Arabidopsis homolog of SWI3, a core subunit of yeast Swi/Snf chromatin remodeling complex, interacts with FCA, a regulator of flowering time. *Nucleic Acids Res.* **30**, 3412–3421 (2002).
24. A. Saez, A. Rodrigues, J. Santiago, S. Rubio, P. L. Rodriguez, HAB1-SWI3B interaction reveals a link between abscisic acid signaling and putative SWI/SNF chromatin-remodeling complexes in Arabidopsis. *Plant Cell* **20**, 2972–2988 (2008).
25. Y. Zhu, M. J. Rowley, G. Böhmdorfer, A. T. Wierzbicki, A SWI/SNF chromatin-remodeling complex acts in noncoding RNA-mediated transcriptional silencing. *Mol. Cell* **49**, 298–309 (2013).
26. W. Han *et al*., The SWI/SNF subunit SWI3B regulates IAMT1 expression via chromatin remodeling in Arabidopsis leaf development. *Plant Sci* **271**, 127–132 (2018).
27. G. P. Leung, L. Lee, T. I. Schmidt, K. Shirahige, M. S. Kobor, Rtt107 is required for recruitment of the SMC5/6 complex to DNA double strand breaks. *J. Biol. Chem.* **286**, 26250–26257 (2011).
28. M. Räschle *et al*., DNA repair. Proteomics reveals dynamic assembly of repair complexes during bypass of DNA cross-links. *Science* **348**, 1253671 (2015).
29. J. Lai *et al*., The transcriptional coactivator ADA2b recruits a structural maintenance protein to double-strand breaks during DNA repair in plants. *Plant Physiol.* **176**, 2613–2622 (2018).
30. J. J. Palecek, SMC5/6: Multifunctional player in replication. *Genes (Basel)* **10**, E7 (2018).
31. D. Yuan *et al*., AtMMS21 regulates DNA damage response and homologous recombination repair in Arabidopsis. *DNA Repair (Amst.)* **21**, 140–147 (2014).
32. A. Georgoulis, C. E. Vorgias, G. P. Chrousos, E. P. Rogakou, Genome instability and γH2AX. *Int. J. Mol. Sci.* **18**, E1979 (2017).
33. H. B. Lindroos *et al*., Chromosomal association of the Smc5/6 complex reveals that it functions in differently regulated pathways. *Mol. Cell* **22**, 755–767 (2006).
34. C. Tapia-Alveal, M. J. O'Connell, Nse1-dependent recruitment of Smc5/6 to lesion-containing loci contributes to the repair defects of mutant complexes. *Mol. Biol. Cell* **22**, 4669–4682 (2011).
35. K. Zabrady *et al*., Chromatin association of the SMC5/6 complex is dependent on binding of its NSE3 subunit to DNA. *Nucleic Acids Res.* **44**, 1064–1079 (2016).
36. K. Jeppsson, T. Kanno, K. Shirahige, C. Sjögren, The maintenance of chromosome structure: Positioning and functioning of SMC complexes. *Nat. Rev. Mol. Cell Biol.* **15**, 601–614 (2014).
37. R. Gómez *et al*., Dynamic localization of SMC5/6 complex proteins during mammalian meiosis and mitosis suggests functions in distinct chromosome processes. *J. Cell Sci.* **126**, 4239–4252 (2013).
38. E. Sarnowska *et al*., The role of SWI/SNF chromatin remodeling complexes in hormone crosstalk. *Trends Plant Sci.* **21**, 594–608 (2016).
39. P. A. Jeggo, J. A. Downs, Roles of chromatin remodellers in DNA double strand break repair. *Exp. Cell Res.* **329**, 69–77 (2014).
40. H. S. Lee, J. H. Park, S. J. Kim, S. J. Kwon, J. Kwon, A cooperative activation loop among SWI/SNF, gamma-H2AX and H3 acetylation for DNA double-strand break repair. *EMBO J.* **29**, 1434–1445 (2010).
41. P. M. Brownlee, C. Meisenberg, J. A. Downs, The SWI/SNF chromatin remodelling complex: Its role in maintaining genome stability and preventing tumourigenesis. *DNA Repair (Amst.)* **32**, 127–133 (2015).
42. S. Venkatesh, J. L. Workman, Histone exchange, chromatin structure and the regulation of transcription. *Nat. Rev. Mol. Cell Biol.* **16**, 178–189 (2015).
43. J. Lai, D. Han, C. Yang, AtMMS21: Connecting DNA repair and root development. *Trends Plant Sci.* **23**, 89–91 (2018).
44. Y. Liu *et al*., The Arabidopsis SUMO E3 ligase AtMMS21 dissociates the E2Fa/DPa complex in cell cycle regulation. *Plant Cell* **28**, 2225–2237 (2016).
45. L. Wang, H. Chen, C. Wang, Z. Hu, S. Yan, Negative regulator of E2F transcription factors links cell cycle checkpoint and DNA damage repair. *Proc. Natl. Acad. Sci. U.S.A.* **115**, E3837–E3845 (2018).
46. S. D. Yoo, Y. H. Cho, J. Sheen, Arabidopsis mesophyll protoplasts: A versatile cell system for transient gene expression analysis. *Nat. Protoc.* **2**, 1565–1572 (2007).
47. S. J. Clough, A. F. Bent, Floral dip: A simplified method for Agrobacterium-mediated transformation of Arabidopsis thaliana. *Plant J.* **16**, 735–743 (1998).
48. Z. J. Lorković *et al*., Compartmentalization of DNA damage response between heterochromatin and euchromatin is mediated by distinct H2A histone variants. *Curr. Biol.* **27**, 1192–1199 (2017).
49. M. Garcia-Hernandez *et al*., TAIR: A resource for integrated Arabidopsis data. *Funct. Integr. Genomics* **2**, 239–253 (2002).
50. K. Clark, I. Karsch-Mizrachi, D. J. Lipman, J. Ostell, E. W. Sayers, GenBank. *Nucleic Acids Res.* **44**, D67–72 (2016).
51. C. Kanz *et al*., The EMBL Nucleotide Sequence Database. *Nucleic Acids Res.* **33**, D29–D33 (2005).